Modeling exposure to airborne metals using moss biomonitoring in cemeteries in two urban areas around Paris and Lyon in France

Emeline Lequy, Caroline Meyer, Danielle Vienneau, Claudine Berr, Marcel Goldberg, Marie Zins, Sébastien Leblond, Kees de Hoogh, Bénédicte Jacquemin

Moss biomonitoring

In cemeteries of urban areas
Lyon (n=51), Paris (n=77)

ICP-MS analysis
14 metals (cadmium, lead...)

Grimmia pulvinata

+ land use data

Geographic information system
Urban, agricultural, or forest areas; roads; altitude; etc.
Publicly available data

+ land use regression modelling

Over 76x63km (Lyon) and 120x101km (Paris)

Example: Cadmium, Paris region

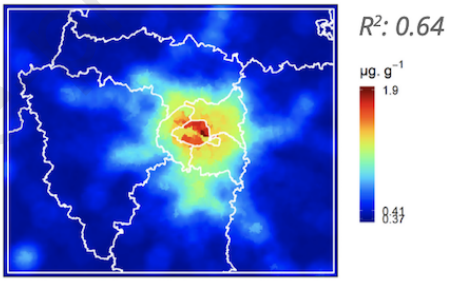

R^2: 0.64

→ Exposure surfaces

Satisfactory for metals emitted by human activities
Plausible exposure surfaces
To be linked with epidemiological data

Modeling exposure to airborne metals using moss biomonitoring in cemeteries in two urban areas around Paris and Lyon in France.

Emeline Lequy1*, Caroline Meyer2, Danielle Vienneau3,4, Claudine Berr5,6, Marcel Goldberg1, Marie Zins1, Sébastien Leblond2, Kees de Hoogh3,4**, Bénédicte Jacquemin7**

1: Unité "Cohortes en Population" UMS 011 Inserm/Université de Paris/Université Paris Saclay/UVSQ, Villejuif, France

2: UMS 2006 Patrimoine Naturel, OFB-CNRS-MNHN, Muséum national d'Histoire naturelle, Paris, France

3: Swiss Tropical and Public Health Institute, Basel, Switzerland.

4: University of Basel, Basel, Switzerland.

5.University of Montpellier, Inserm, INM (Institute of Neurosciences of Montpellier) U1198, Montpellier, France

6. Memory Research and Resources Center, Department of Neurology, Montpellier

7: Univ Rennes, Inserm, EHESP, Irset (Institut de recherche en santé, environnement et travail) – UMR_S 1085, Rennes, France

*: address correspondance to :

Emeline Lequy, UMS 011, Hôpital Paul Brousse, 16 avenue Paul Vaillant Couturier, 94807 VILLEJUIF CEDEX, France. Telephone number: +33 (0)1 77 74 74 19.

E-mail Address: e.lequy@gmail.com

**: equal contribution

Abstract

Exposure of the general population to airborne metals remains poorly estimated despite the potential health risks. Passive moss biomonitoring can proxy air quality at fine resolution over large areas, mainly in rural areas. We adapted the technique to urban areas to develop fine concentration maps for several metals for Constances cohort's participants. We sampled *Grimmia pulvinata* in 77 and 51 cemeteries within ~50km of Paris and Lyon city centers, respectively. We developed land-use regression models for 14 metals including cadmium, lead, and antimony; potential predictors included the amount of urban, agricultural, forest, and water around cemeteries, population density, altitude, and distance to major roads. We used both kriging with external drift and land use regression followed by residual kriging when necessary to derive concentration maps (500x500m) for each metal and region. Both approaches led to similar results. The most frequent predictors were the amount of urban, agricultural, or forest areas. Depending on the metal, the models explained part of the spatial variability, from 6% for vanadium in Lyon to 84% for antimony in Paris, but mostly between 20% and 60%, with better results for metals emitted by human activities. Moss biomonitoring in cemeteries proves efficient for obtaining airborne metal exposures in urban areas for the most common metals.

Keywords: air pollution; moss biomonitoring; cadmium; lead; exposure surface; land-use regression

Introduction

As naturally occurring elements, metals abundantly occur in the lithosphere and accumulate in the biosphere and atmosphere through processes including root absorption and subsequent transfer through food webs, wind erosion, and human activities since the Bronze Age (Gall et al., 2015; Gnesin, 2013; Jaworowski et al., 1981). Some metals support life, yet all become toxic when exceeding thresholds (Nordberg et al., 2007). Cadmium (Cd) and arsenic (As) for example are recognized human carcinogens (International Agency for Research on Cancer, 2016), and, as neurotoxicants, lead (Pb) and mercury (Hg) may also play a role in the development and decline of cognitive functions (Genuis and Kelln, 2015; Grandjean and Landrigan, 2014). As early as the 1960s it's been known that airborne metals are a component of airborne particulate matter (PM) (Schroeder, 1968), and it is also established that air pollution also affects health and cognition (Brauer et al., 2012; Gatto et al., 2014). In Europe, toxic metals As, Cd, Pb, and nickel (Ni), have been measured in PM (diameter<10μm or PM10) as enforced by Council Directive 96/62/EC of 27 September 1996 on ambient air quality assessment and management and its updates. Yet these measurements are performed only at a few sites, providing insufficient spatial coverage to allow for assessing the exposure of the general population to these airborne metals. Further, the directive does not include other potentially harmful metals such as aluminum (Al), antimony (Sb), copper (Cu), or zinc (Zn).

In France, a network of moss biomonitoring of atmospheric deposition of metals on mosses (BRAMM) has recorded metal concentrations in mosses across 400-500 sampling sites over the rural and forested areas since 1996 (Lequy et al., 2016) following the guidelines of the international program ICP-Vegetation (Schröder et al.,

2016). Briefly, this moss-biomonitoring technique, detailed in (Markert, 2007), relies on mosses' lack of roots, making them dependent on atmospheric sources to get water and nutrients (Bates, 1992; Tyler, 1990). Mosses combine a morphology of leaves able to trap particulate metals (Bargagli, 2006) to a monolayer cell thickness facilitating the accessibility of dissolved metals for the exchange sites in the cell walls (Bates, 1992; Carballeira et al., 2008; González and Pokrovsky, 2014). Data obtained by this technique allowed for deriving concentration maps suitable for the French rural and semi-urban populations, and was successfully used to estimate mortality risks associated to airborne metal exposure (Lequy et al., 2019). However, most of the French population lives in urban areas for which the above-mentioned concentration maps are not suitable. In fact, to the best of our knowledge, there are no available fine concentration map for metals for urban populations. Moss biomonitoring was shown to perform well in urban areas (Gallego-Cartagena et al., 2021; Jiang et al., 2018; Zechmeister et al., 2005), capturing particles mostly within the inhalable fraction (Di Palma et al., 2017), and with a large influence of urban or traffic land use variables on metal concentrations in mosses (De Nicola et al., 2013; Di Palma et al., 2017) but with a negligible contribution of soil on metal concentrations (Jiang et al., 2018). Specific sources of metals are well known, such as non-exhaust traffic (e.g. brakes) for Cu, Sb or Pb, or local or distant steel industry for Cd (Ledoux et al., 2017). For these reasons, we aimed at adapting the moss biomonitoring technique to urban settings to derive fine concentration maps by land use regression (LUR) modelling in two of the most populated French regions, the greater Paris and Lyon areas.

Material and Methods

To adapt the technique of moss biomonitoring used by BRAMM (Harmens, 2010) to urban areas, we needed to find suitable sampling sites and moss species. Regarding

sampling sites, we opted for cemeteries for several reasons: at least one is located in most municipalities, they can shelter mosses (Natali et al., 2016), cemeteries in urban municipalities are near sources of air pollutants such as roads while being relatively sheltered from direct contamination by humans or animals, and they offer homogeneous substrates such as concrete. In addition, opting for cemeteries allows for collecting mosses that grow in full light and can survive in contaminated environments. We selected a moss living in cushion, *Grimmia pulvinata* (Hedw.) Sm., which performs well in biomonitoring airborne metals (Gallego-Cartagena et al., 2021), including in cemeteries (Natali et al., 2016).

Study design

With the goal to provide concentration maps for urban populations for the general population-based Constances cohort (Zins et al., 2015), the sampling strategy was designed to cover the widest urban area where Constances participants were residing and in which we could find cemeteries to sample mosses. To do so, and to obtain sampling sites as evenly distributed as possible to subsequently develop an concentration map, we proceeded as follows.

We developed a “target-style” gridded study design (Figure 1), with concentric circles around the city center with increasing radii up to 49km around Paris and 30km around Lyon. These circles were crossed by transects starting from the center of the study site and passing through areas with the highest possible population density, while covering as many directions as possible. We classified population density into categories based on two indexes defined by the French institute for Statistics, according to the size of the municipality (Institut national de la statistique et des études économiques (National Institute of Statistics and Economic Studies), n.d., n.d.). For municipalities with less than 5000 inhabitants, the index is high, moderate,

low, and very low population density, taking into account the surface actually inhabited. For municipalities with more than 5000 inhabitants, the index is residential, commercial or industrial areas, and recreational areas. In Figure 1, to improve readability, the municipalities with less than 5000 inhabitants with high population density and the residential areas of municipalities with more than 5000 inhabitants were merged into a “high” population density category, and the low and very low population density areas of municipalities with less than 5000 inhabitants into a “low” population density category. In the areas around Paris and Lyon and their surrounding areas (referred to as Paris and Lyon for readability), population density decreases as the distance from city center increases, therefore reaching low values in the outer circles. The junctions between circles and transects defined different potential sampling sites. The absence of cemeteries at some junctions, the refusal of the town halls to collect mosses in cemeteries, the absence of concrete walls or tombstones, or the species of mosses have led to modify the initially selected sampling sites. Final sampling sites were chosen in the field among the potential candidates matching our criteria: 77 sites in Paris, 51 sites in Lyon.

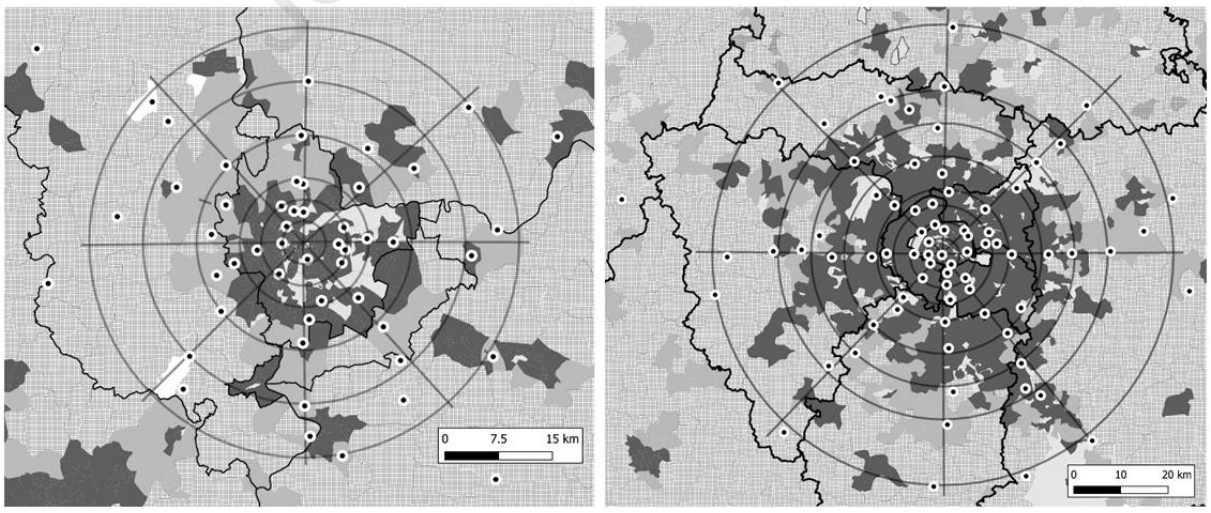

Figure 1: distribution of sampling sites (white-circled black dots) around Lyon (left) and Paris (right). Dark gray, medium gray, and gridded-gray areas

141 indicate high, intermediate, and low population densities. Pale gray areas correspond
142 to business or industry parks and to large uninhabited areas (forests, large parks,
143 airports). Black lines indicate the borders of French départements.
144

145 ## Moss sampling and metal concentrations

146 Details of the moss sampling are available in Vieille et al (2021). Briefly, sampling in
147 the Paris and Lyon regions took place in May and June 2018, respectively. In each
148 sampling site, mosses were sampled with standardized methods by trained experts
149 only on concrete substrate, either on tombstones or on the top of walls, as follows: we
150 collected an average of 75 moss colonies (minimum 50), on at least 10 tombstones or
151 on a total length of 15m of top of wall, and using two different walls, to reduce the
152 influence of any moss cushion potentially contaminated by the substrate. We chose
153 concrete because of the low risk of potential contamination. Moreover, we avoided
154 decorative metallic objects. Sampling collection in each site included a total of about
155 9600 cushions. Each cushion was validated with a magnifying glass (10x
156 magnification). Samples were stored in a cooler before being brought back in the
157 laboratory where they dried at room temperature before being manually cleaned,
158 ground with an automatic non-polluting titanium grinder (Pulverisette 14, Fritsch,
159 Germany), and sent for analyses. Sampling and preparation were conducted using
160 nytril gloves and ceramic knives to avoid contamination. Mosses were analyzed by
161 inductively coupled plasma mass spectrometry by the USRAVE laboratory (INRAE-
162 Centre de Bordeaux) (Agilent 7700x spectrometer) after drying at 40°C and acid
163 mineralization by HF/HNO3/H2O2 (concentrations expressed at 103°C after
164 accounting for water loss on a subsample). For Hg, the moss powder is directly
165 analyzed by Cold Vapour Atomic Fluorescence Spectrometry. Analyses provided
166 concentrations of aluminum (Al), arsenic (As), calcium (Ca), cadmium (Cd),

chromium (Cr), Cu, iron (Fe), mercury (Hg), sodium (Na), nickel (Ni), lead (Pb), antimony (Sb), vanadium (V), and zinc (Zn). Analytical uncertainties are 20% for As, Cd, Cr, Cu, Na, Ni, Pb, Sb and V, 15% for Al and Fe and 10% for Ca, Hg and Zn.

Generating concentration maps

Source data for potential predictors

Corine Land Cover (2018, on https://www.copernicus.eu/en) was used to calculate the relative coverage of urban area, agricultural area, forest area, natural area, water within buffers of 500, 1000, 2500, and 5000 m radius around the sampling site (the subcategories used to define each category are detailed in the supplementary material). We used a minimal buffer radius of 500m due to the resolution of Corine Land Cover (250x250m). Sata from the French GIS database (Institut Géographique National) were used to calculate distance from major roads (defined as those classified level 1 and 2 i.e. corresponding to highways or equivalent, access roads, and other busy roads - in m), the population density of each municipality (in inhabitant/km^2), and the altitude (in m). To consider the potential influence of industry, we used the European pollutant release and transfer register for industrial emissions (in the air only and in 2018) to calculate, for each available metal (As, Cd, Cr, Cu, Hg, Ni, Pb, and Zn) the distance to the closest industrial site (in m) and the total annual emissions released by this site (in kg).

To use the most informative variables that did not risk to provide distorted estimates in the models, we removed any predictor containing more than 50% of null values before starting developing the LUR models (Table 1).

All GIS processing and analyses were performed with R version using the packages "SP"(Bivand et al., 2013), "RASTER"(Hijmans, 2020), "GSTAT"(Gräler et al., 2016), and "AUTOMAP"(Hiemstra et al., 2008).

Table 1: list of variables and their description.

Type	Variable	Buffer size (radius, m)	Code	N(%) or median [p25, p75] Lyon (n=51)	Paris (n=77)
Point	Substrate: wall or tombstone*	-	Substrate(Tombstones)	9 (18%)	58 (82%)
	Altitude (m)	-	altitude	259 [216, 316]	78 [51, 110]
	Population density (inhab/km²)	-	density	370 [166, 1979]	1804 [247, 7997]
	Distance to major roads (m)	-	dist_road	925 [419, 1857]	530 [210, 1334]
Buffer (%)	agricultural area within:	500	agri_500	34 [0, 55]	0 [0, 37]**
		1000	agri_1000	40 [6, 69]	10 [0, 47]
		2500	agri_2500	53 [23, 67]	15 [0, 53]
		5000	agri_5000	52 [24, 67]	19 [1, 52]
	forest area within:	500	forest_500	0 [0, 4]**	0 [0, 5]**
		1000	forest_1000	0 [0, 12]**	3 [0, 20]
		2500	forest_2500	8 [0, 18]	9 [0, 22]
		5000	forest_5000	10 [4, 15]	14 [1, 26]
	urban area within:	500	urb_500	63 [42, 91]	90 [49, 100]
		1000	urb_1000	50 [24, 86]	68 [28, 100]
		2500	urb_2500	33 [10, 73]	60 [16, 95]
		5000	urb_5000	28 [13, 69]	52 [17, 95]
	water area within:	500	water_500	0 [0, 0]**	0 [0, 0]**
		1000	water_1000	0 [0, 0]**	0 [0, 0]**
		2500	water_2500	0 [0, 4]**	0 [0, 2]**
		5000	water_5000	2 [0, 4]	1 [0, 3]

*: only concrete tombstones and top of walls

**: removed from dataset before developing the land use regression models. Natural area (see supplementary material for the details) buffer variables all included more than 50% of null values and were deleted from the dataset. p25 and p75 stand for the 25th and 75th percentiles.

Developing land use regression models

LUR models were developed separately in each region. We aimed to find the most parsimonious models with the best goodness of fit between metal concentrations in mosses and spatial predictors, and applied the following steps. We natural log-

transformed metal concentrations when the distribution was left-skewed, and checked for any outlier. We found only one outlier, for Hg in the Paris region, with an unlikely value of 1 $\mu g.g^{-1}$, which we excluded. After computing univariate Spearman correlations between each metal concentration and all spatial predictors, we pre-selected only variables with a Spearman correlation coefficient>0.3. We used supervised modeling to choose the final predictors, after conducting both forward and backward stepwise approaches. At first, we used generalized additive modeling to account for any possible nonlinear relationship by including spline functions for all continuous variables.

Forward stepwise approach: for each metal, we included potential predictors one by one in a generalized additive model. Starting from the predictor yielding the univariate model with the highest R2, followed by the next highest in turn. At each iteration we kept the newly included predictor only if the variable increased the adjusted R2 of the multivariate model.

Backward stepwise approach: for each metal, we included all the variables with a statistically significant Spearman correlation coefficient>0.3. For both approaches, we subsequently removed one by one any variable with a p-value>0.05. When all the remaining variables were significantly associated with the metal concentration, we handled nonlinear relationship as follows: when the predictor had more than 1 degree of freedom (i.e. a nonlinear relationship), and if the relationship visually did not deviate too much from linearity, we simply removed the spline function. If the relationship visually deviated from linearity, but was monotonic or transformable, we replaced the spline function by the most suitable function (power or natural logarithm). In the case of a non-monotonic and not easily transformable relationship, we removed the variable from the model. We also checked whether the relationship was in the expected direction. Finally, for each model we compared the models

yielded by the forward and backward approaches and selected as final model the one with the best adjusted R2.

Deriving concentration maps

We created a 500x500m resolution grid covering each region and computed all the predictors used by the final models for each metal on each mesh of these grids to generate the concentration maps. We then applied, on each 500x500m mesh of these grids, the final models based on two methods, to generate concentration maps: kriging with external drift (KED) or land use regression (LUR) followed by residual kriging when necessary. Regarding KED, for each metal in each region, a variogram was computed, based on the site geocodes, the metal concentration (log-transformed when necessary), and the predictors included in the final model (Figure S1). Using this modelled variogram, universal kriging was performed over the 500m pixels. Regarding LUR with kriging of the residuals, for each metal in each region, we applied the final model over the 500x500m grid. Then, when the residuals of the final model showed a statistically significant spatial autocorrelation based on Moran's I test (Bivand et al., 2013), we performed ordinary kriging over the 500x500m grid and added these values to those obtained after applying the LUR model.

Quality of the models and of the concentration maps.

To estimate the quality of each final model, in addition to the adjusted R2, we computed the Akaike Information Criterion (AIC) and the variance inflation factor (VIF) of each variable of each model. We considered multicollinearity for VIF larger than 10. We assessed the quality of KED and LUR by 10-hold out validation (10-HOV). For each metal, separately in each study area, we first used 10 training sets (each set is a random selection of 90% of the sites) to derive regression coefficients

for both approaches, and to obtain variograms for all metals in the KED approach. We then applied the coefficients and variograms to generate maps over the 500x500m grid. We back-transformed the predicted values for all the natural log-transformed metals. Additionally, we developed variograms of the residuals from the LUR models using the training sets. We performed a 10-HOV first to evaluate the robustness of the final model, and another 10-HOV to evaluate the robustness of the variogram for the residual kriging. Finally, we extracted the predicted values at the coordinates of the validating sets (the remaining 10% of sites) and regressed these predicted values on the corresponding observed values to obtain a R2; we also calculated the relative root mean square error (RRMSE). We categorized modeling quality scores: 1 (satisfactory final model (adjusted R2>0.45) with satisfactory robustness (quantified by 10-HOV with an R2>0.3)), 2 (satisfactory final model with poor robustness or conversely), and 3 (poor final model with poor robustness).

Results

Metal concentrations

In both regions combined, metal concentrations ranged over several orders of magnitudes from Hg to Ca, between 0.10 $\mu g.g^{-1}$ [IQR: 0.21] for Hg and 1.7 10^4 $\mu g.g^{-1}$ [IQR: 2.3 10^4] for Ca (Figure 2). The magnitude was similar for each metal in the two regions, but still we found concentrations of Cd, Cu, Pb, Sb, and Zn at least twice as high in Paris as in Lyon.

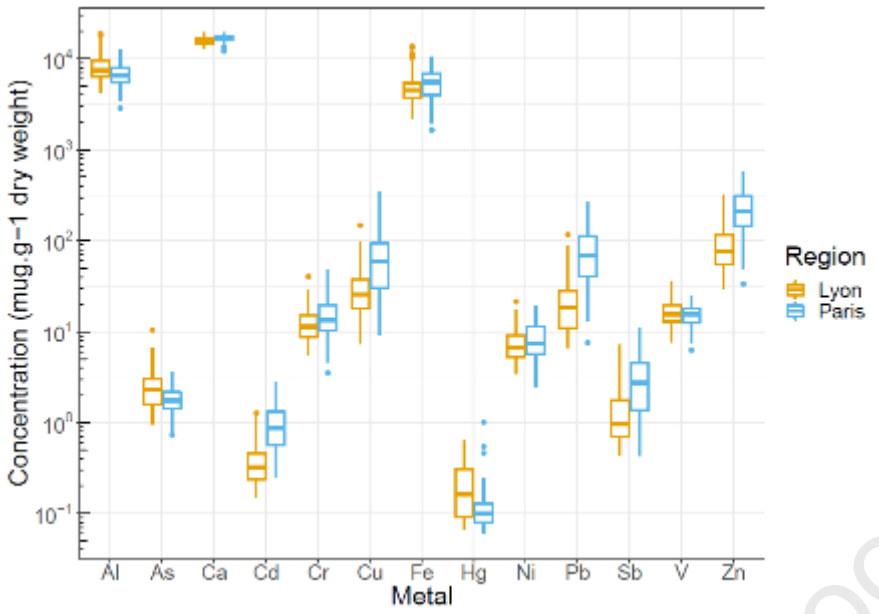

Figure 2: distribution (Y-axis on a log-10 scale) of the metal concentrations in mosses collected in the cemeteries of the regions of Lyon (n=51) and Paris (n=77) in 2018. See Table S1 for corresponding numeric data.

Final models

Most final models were constructed based on the backward stepwise selection, which provided slightly higher adjusted R2 for more than half of the metals in both regions (Table S2). Depending on the metal, and on the region, the models explained part of the spatial variability, from 6% for vanadium in Lyon to 84% for antimony in Paris, but mostly between 21%-54% in Lyon and 30-60% in Paris, with better results for metals emitted by human activities (Table 2). For each metal in both study regions, final models yielded lower AIC than intercept-only models (Table S3). The models yielded relationships in the expected direction for each included predictor (such as higher concentrations of metals with higher coverage of urban areas, population density, or closer to major roads) (Table 2). The final models typically explained more

291 variance in Paris, except for Al and As. Residuals were spatially autocorrelated only
292 for Ca, Na, and Ni in Lyon.
293 In each final model, the VIF of most predictors was lower than two, with only some
294 values larger than six but overall indicating no multicollinearity (Table S4).
295
296 **Table 2: final models for each metal in each region, including the**
297 **transformation of the metal distribution, the formula used for the linear**
298 **regression, and the adjusted R2.**
299

Region	Metal	Transformation	Model formula	R2
Lyon	Al	natural log	6.9 + forest_2500 x -1.4 + I(dist_road^-0.05) x 2.7 + altitude x 0.0013	0.26
Paris	Al	none	7600 + forest_5000 x -5800	0.24
Lyon	As	natural log	0.51 + forest_2500 x -2.9 + altitude x 0.0023	0.37
Paris	As	none	2.1 + forest_5000 x -1.8	0.25
Lyon	Ca	none	15000 + urb_1000 x 1700	0.14
Paris	Ca	none	17000 + agri_5000 x -1700 + density x 0.06 + forest_1000:I(forest_1000 < 0.25) x -690 + forest_1000:I(forest_1000 ≥ 0.25) x 7400	0.28
Lyon	Cd	natural log	-1 + urb_1000x0.59 + I(forest_5000^0.3) x -0.93 + Substrate(Tombstones) x 0.38	0.58
Paris	Cd	natural log	-1 + urb_5000 x 0.87 + density x 2e-5 + Substrate(Tombstones) x 0.34	0.67
Lyon	Cr	natural log	2.7 + forest_2500 x -2.1	0.31
Paris	Cr	natural log	2.8 + altitude x -0.0033 + urb_5000 x 0.44 + forest_2500 x -1.1	0.63
Lyon	Cu	natural log	3.1 + urb_1000 x 0.9 + forest_2500 x -2.1	0.55
Paris	Cu	natural log	3 + urb_5000 x 1.6 + water_5000 x 7.2	0.67
Lyon	Fe	natural log	8.7 + forest_2500 x -1.7	0.20
Paris	Fe	none	1700 + altitude x -13 + urb_5000 x 6500 + agri_5000 x 5000	0.50
Lyon	Hg	natural log	-2.3 + urb_1000 x 0.99	0.23
Paris	Hg	natural log	-2.9 + altitude x -0.0025 + urb_2500 x 0.95 + agri_5000 x 0.81 + Substrate(Tombstones) x 0.2	0.34
Lyon	Na	natural log	7 + forest_2500 x -1.8	0.12

Paris	Na	natural log	6.5 + forest_2500 x -1.1 + agri_2500 x 0.33	0.29
Lyon	Ni	natural log	1.9 + urb_1000 x 0.38 + forest_2500 x -1.3	0.32
Paris	Ni	natural log	2.1 + altitude x -0.0031 + urb_500 x 0.27 + forest_2500 x -1.1 + density x 1.5e-05 + Substrate(Tombstones) x 0.16	0.69
Lyon	Pb	natural log	2.1 + urb_500 x 1.1 + Substrate(Tombstones) x 0.72	0.49
Paris	Pb	natural log	3.4 + forest_1000 x -1.2 + density x 3.7e-05 + Substrate(Tombstones) x 0.91	0.59
Lyon	Sb	natural log	1.5 + agri_1000 x -0.75 + I(forest_5000^0.2) x -1.8	0.62
Paris	Sb	natural log	0.16 + urb_5000 x 1.6 + forest_1000 x -1.2	0.84
Lyon	V	natural log	2.9 + forest_5000 x -0.88	0.06
Paris	V	none	-0.75 + urb_5000 x 15 + agri_5000 x 15 + I(altitude^-0.5) x 34	0.43
Lyon	Zn	natural log	6.5 + I(forest_5000^0.3) x -2.2 + agri_500 x -0.92 + log(density) x -0.12	0.65
Paris	Zn	natural log	4.5 + urb_5000 x 0.61 + density x 2.8e-05 + Substrate(Tombstones) x 0.47	0.56

On average, the final models included approximately three predictor variables in Paris and two in Lyon (Table S5). In both regions, the most frequent covariables were forest and urban land use – they occurred even more frequently in Lyon than in Paris; population density entered more frequently in the Paris models (Table 1). The large majority of predictors had linear relationships with metal concentrations and did not need transformation, with a few exceptions such as forest and population density for Zn in Lyon (Table 2).

Comparing the mapping approaches in the two regions

The LUR approach needed a further step of residual kriging only for Ca, Na, and Ni in the Lyon region. The 10-HOV indicated that this supplementary step increased the quality of the modelling for Ca and Ni, but not for Na. Using the same final models for both KED and LUR, the 10-HOV yielded similar R2 for both approaches and most metals (Table 3). The HOV-10 R2 ranged from 0.03 to 0.74, and the RRMSE ranged between 0.08 to 0.88. Comparing the adjusted R2 of the final models to those of the 10-HOV, we calculated lower absolute values of percentage change in Paris (median

317 14%, IQR 6-40) than in Lyon (median 38%, IQR 12-45) and therefore varying
318 robustness across metals and areas. Combining this estimation of robustness and the
319 amount of explained spatial variation by the final models, we broadly classified three
320 types of modelling quality: satisfactory adjusted R2 of the final model with
321 satisfactory robustness (eg Zn in Lyon), satisfactory adjusted R2 of the final model
322 with poor robustness (eg Pb in Paris) or poor adjusted R2 of the final model with
323 satisfactory robustness (eg As in Lyon), and poor adjusted R2 of the final model with
324 poor robustness (eg Na in Lyon) (Table 3).
325

326 **Table 3: R2 and RRMSE (unitless) of the HOV-10 validation for the KED**
327 **and LUR approaches, and final approach chosen as the one providing the**
328 **higher R2.**

Metal	Region	R2			RRMSE		Final approach	Model quality
		HOV10, KED	HOV10, LUR		HOV10, KED	HOV10, LUR		
			Model	Kriging				
Al	Lyon	0.05	0.20		0.46	0.41	LUR	3
Al	Paris	0.18	0.22		0.20	0.20	LUR	3
As	Lyon	0.39	0.28		0.43	0.47	KED	2
As	Paris	0.17	0.20		0.28	0.28	LUR	3
Ca	Lyon	0.10	0.05	0.08	0.09	0.09	KED	3
Ca	Paris	0.09	0.12		0.08	0.08	LUR	3
Cd	Lyon	0.31	0.34		0.51	0.46	LUR	1
Cd	Paris	0.33	0.36		0.56	0.54	LUR	1
Cr	Lyon	0.20	0.21		0.52	0.52	LUR	3
Cr	Paris	0.60	0.62		0.27	0.26	LUR	1
Cu	Lyon	0.30	0.30		0.71	0.71	LUR	1
Cu	Paris	0.50	0.52		0.46	0.44	LUR	1
Fe	Lyon	0.14	0.17		0.50	0.49	LUR	3
Fe	Paris	0.47	0.46		0.25	0.25	KED	1
Hg	Lyon	0.17	0.15		0.67	0.67	KED	3
Hg	Paris	0.22	0.41		0.31	0.22	LUR	2
Na	Lyon	0.04	0.07	0.02	0.80	0.81	KED	3
Na	Paris	0.06	0.08		0.31	0.3	LUR	3
Ni	Lyon	0.38	0.26	0.35	0.41	0.42	KED	2
Ni	Paris	0.63	0.64		0.34	0.34	LUR	1

Pb	Lyon	0.03	0.08	0.88	0.83	LUR	2
Pb	Paris	0.17	0.20	0.75	0.76	LUR	2
Sb	Lyon	0.27	0.31	0.87	0.81	LUR	1
Sb	Paris	0.71	0.74	0.37	0.36	LUR	1
V	Lyon	0.03	0.03	0.41	0.41	LUR	3
V	Paris	0.51	0.53	0.16	0.16	LUR	2
Zn	Lyon	0.47	0.48	0.54	0.52	LUR	1
Zn	Paris	0.29	0.34	0.53	0.54	LUR	1

HOV: hold-out validation; LUR: land use regression ; KED: kriging with external drift. For the LUR approach, metals Ca, Na, and Ni required an extra step of residual kriging since the residuals of the regression had a significant positive spatial autocorrelation. Modeling quality scores: 1 (satisfactory final model (adjusted R2>0.45) with satisfactory robustness (quantified by 10-HOV with an R2>0.3)), 2 (satisfactory final model with poor robustness or conversely), and 3 (poor final model with poor robustness).

329

330 Final concentration map by metal and by region

331 The final concentration map for each metal and each region is the one with the higher
332 adjusted R2 and lower RRMSE after 10-HOV (Table 3). The LUR approach was
333 favoured for most metals in both regions. The predicted concentration maps clearly
334 show the gradual decline on concentration away from the city center. This pattern is
335 driven by the urban and natural predictor variables entering in most models (Figure
336 3, Figure S2).

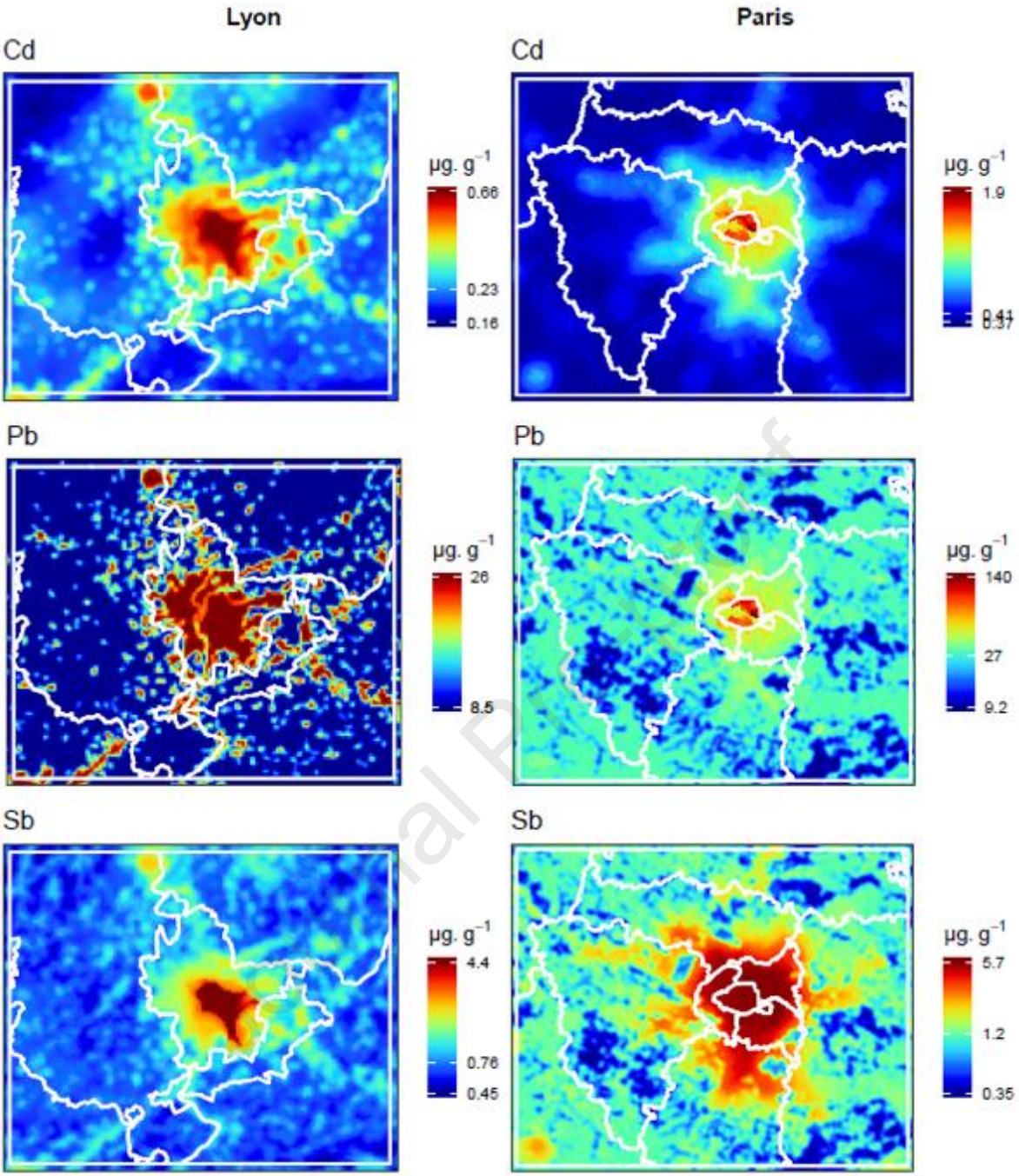

337

338 **Figure 3: final concentration maps of Cd, Pb, and Sb in Lyon (left) and**

339 **Paris (right).** The legends display the minimum, median and maximum values on a

340 log-10 scale for readability. These maps have the same extents as those in Figure 1.

341 White lines represent the borders of French départements.

Discussion

Biomonitoring of mosses in cemeteries together with geostatistical modelling proved an efficient method to generate concentration maps in urban areas, with satisfactory quality for metals emitted by human sources, such as Cd and Cu, but with lesser quality for metals emitted by natural sources, such as Ca and Na. The final models were parsimonious. In most cases, KED and LUR modelling yielded similar results but with generally better robustness for LUR.

To date, only few other methods allow attributing airborne metal exposures to populations. CHIMERE, a chemistry-dispersion model, provides concentrations of PM and PM components regionally (Mailler et al., 2017; Menut et al., 2013) and showed some agreement in the predicted concentrations of atmospheric Cd and measured concentrations of Cd in mosses, with Kendall correlations generally above 0.5 in Paris and 0.4 in Lyon (Vieille et al., 2021). LUR models have been developed for some metals included in PM2.5 in Western Europe (Chen et al., 2020), and in Pittsburgh, USA (Tripathy et al., 2019). A GIS-based tool provides Cd exposure from industrial sources (Coudon et al., 2019), but only from industrial sources and not yet for other metals. A study using field X-Ray analysis on epiphytic mosses to measure Cu, Pb, and Zn, also produced LUR maps in a study area in the USA but for three metals (Messager et al., 2021). Studies comparing or combining these predicted exposures would help better estimate exposure to airborne metals. There were not enough monitoring sites of concentrations of metals (As, Cd, Ni, Pb) in PM10 to allow for a comparison with our exposure assessment, again advocating for more measuring sites or alternative measurement techniques.

This study is based on passive moss biomonitoring, whose concentration values show strong relationships with modelled metal emission or deposition in rural areas at least for Cd and Pb (Harmens et al., 2012), and of Cd in Paris and Lyon (Vieille et al., 2021). This moss biomonitoring technique, which therefore can proxy atmospheric concentrations, allowed for (i) rapid collection of sufficient moss samples to cover large urban areas and (ii) measuring many metals or potential other components (e.g. persistent organic pollutants, platinoids) with high cost-effectiveness. Cemeteries – at least in France – offer a regular sampling frame and choice of possible sampling sites that will most likely shelter *Grimmia pulvinata*, or, at least, a single moss species that will not risk to confound the spatial variability of the measured concentrations. For the sake of homogeneity and to avoid potential contamination by debris of different substrates, we sampled only concrete surface. Regarding the modeling process, all the predictors used to build the final models were readily available and open source, with regular updates so that the predictor data generally matched the moss sampling periods. The sets of final predictors were quite similar in both regions even though population density entered more frequently in the Paris models, probably due to the high percentages of urban coverage and the high variability in population density in Paris. However, for each metal both variables and coefficients differed between the two regions; more data in other regions is needed to explore the possibility to pool the data to obtain a single model to be applied to several unsampled regions. None of the models used the data on industrial sites, probably because they were too far from the sampling sites in both regions with at least a few kilometres from the closest site. The final models explained a large amount of the spatial variability of metals mainly emitted by human activities except Hg, with between 40 and 82% explained for Ni in Lyon or Sb in Paris, respectively. At ambient temperature Hg can exist in gaseous form, and this high volatility may have

disturbed the spatial distribution of Hg concentrations in mosses collected during late spring. During the sampling, temperatures were as high as 27.2°C and 28.6°C in Paris and Lyon (data from the French meteorological agency MeteoFrance) – without considering the likely higher temperature on the concrete substrate. For metals mostly emitted by natural sources, the models explained a lesser amount of spatial variability. We did not detect strong multicollinearity in the final models. Some VIF values larger than 6 occurred in models including both urban and agriculture or forest variables, which were negatively correlated. However, multicollinearity does not affect the models' predictive accuracy.

The present result showed largely higher moss concentrations in urban areas than those previously found in rural areas since 1996 (Lequy et al., 2017), up to a factor 12 for Cu for example, in Paris. These urban and rural results seem consistent and plausible, given the positive relationships of metals with relative urban area or negative relationships with its opposite, i.e. greenspace areas, and a strong gradient from the city center to the rural outskirts of Lyon and Paris, and in line with other studies. Indeed, despite the methods are not the same and therefore the estimates are not straightforwardly comparable, the relationships we found between metal concentrations and land used variables, such as traffic, were of the same direction as those found in studies using field measurements on epiphytic mosses in the USA (Messager et al., 2021), or using other biomonitoring techniques using moss bags or epiphytes in Italy (Capozzi et al., 2016; Di Palma et al., 2017). All of these techniques were able to capture spatial variations of metals from either urban or rural sources, thereby reinforcing the plausibility of our results. In our dataset, forest and agricultural variables were negatively correlated with urban variables and may better capture the variability of some metals in mosses in cemeteries.

This study presents the limits inherent to passive moss biomonitoring, including the uncertainty on the period of exposure they represent. However, it is usually estimated that mosses accumulate metals over their lifespan of several years. Mosses, being living organisms, are affected by meteorological conditions in particular drought periods since mosses rely on water even more than other plants (Markert, 2007). But since they accumulate over several years, we took the hypothesis, as in the BRAMM network and the ICP-Vegetation program, that the concentrations in mosses are able to reflect spatial variations in air quality when compared across sampling sites for the same date. Several possible disturbances may either disturb mosses' physiology and their ability to biomonitor metals, or contaminate mosses with metals: the use of bleach or surfactants to clean tombstones, or the (former) paintings on some tombstones, which cannot be easily retrieved, or the use of herbicides or other products by cemeteries. During the sampling, data on the use of herbicides or other products proved difficult to collect, with information available for 55% and 80% of the sampled cemeteries in the regions of Paris and Lyon, respectively. Of those, 29% and 47% had information while 26% and 33% declared they used no treatment, in the respective study areas. We could not assess the local effect of wind-blown particles of cemeteries' topsoil, possibly contaminated by metals (Neckel et al., 2016); yet the spatial patterns of metal concentrations, and their relationships with the land use variables included in the final models, suggest that any local topsoil effect would be negligible . The fact that *Grimmia pulvinata* develops preferentially on concrete does not allow the use of cemeteries or tombstones built in a material other than concrete (e.g. granite). This was not an issue in Paris or Lyon but it may be the case in other regions in France or in the world, for which it would be mandatory to find a more suitable moss species. As expected, KED and LUR provided similar maps of similar quality; KED may be used as an alternative for air pollutants when using LUR does

not provide satisfactory outputs. The 10-HOV indicated that some models lack robustness but the concentration maps presented in this study showed plausible spatial patterns, at least for metals emitted by human activities. Such concentration maps seem to provide a sufficient geographical contrast in concentrations across each study area, for a future use as exposure data at individual level in epidemiological studies.

Conclusion

Moss biomonitoring in cemeteries offers a practical alternative for rapid estimation of exposure to airborne metals in urban areas, and land-use regression provided satisfactory concentration maps for airborne metals emitted by human sources. Further research to compare these results with more conventional techniques should refine exposure assessment for airborne metals such as Cd, Hg, or Pb, but also for other potentially harmful metals and other pollutants.

Acknowledgements

This study was funded by ANR (ANR-17-CE36-0005) and by Fondation de France (Engt 00089829). The Constances Cohort Study is supported and funded by the Caisse nationale d'assurance maladie (CNAM). The Constances Cohort Study is an "Infrastructure nationale en Biologie et Santé" and benefits from a grant from ANR (ANR-11-INBS-0002) and from the Ministry of Research. Constances is also partly funded by MSD, and L'Oréal. We are grateful to all the municipalities that granted us permission to sample mosses in their cemeteries, and to Nora Rouillier for her help in preparing the samples.

References

Bargagli, R., 2006. Antarctic Ecosystems: Environmental Contamination, Climate Change, and Human Impact. Springer Science & Business Media.

Bates, J.W., 1992. Mineral nutrient acquisition and retention by bryophytes. Journal of Bryology 17, 223–240. https://doi.org/10.1179/jbr.1992.17.2.223

Bivand, R.S., Pebesma, E., Gomez-Rubio, V., 2013. Applied spatial data analysis with R, Second edition. Springer, NY.

Brauer, M., Amann, M., Burnett, R.T., Cohen, A., Dentener, F., Ezzati, M., Henderson, S.B., Krzyzanowski, M., Martin, R.V., Van Dingenen, R., van Donkelaar, A., Thurston, G.D., 2012. Exposure assessment for estimation of the global burden of disease attributable to outdoor air pollution. Environ Sci Technol 46, 652–660. https://doi.org/10.1021/es2025752

Capozzi, F., Giordano, S., Di Palma, A., Spagnuolo, V., De Nicola, F., Adamo, P., 2016. Biomonitoring of atmospheric pollution by moss bags: Discriminating urban-rural structure in a fragmented landscape. Chemosphere 149, 211–218. https://doi.org/10.1016/j.chemosphere.2016.01.065

Carballeira, C.B., Aboal, J.R., Fernández, J.A., Carballeira, A., 2008. Comparison of the accumulation of elements in two terrestrial moss species. Atmospheric Environment 42, 4904–4917. https://doi.org/10.1016/j.atmosenv.2008.02.028

Chen, J., de Hoogh, K., Gulliver, J., Hoffmann, B., Hertel, O., Ketzel, M., Weinmayr, G., Bauwelinck, M., van Donkelaar, A., Hvidtfeldt, U.A., Atkinson, R., Janssen, N.A.H., Martin, R.V., Samoli, E., Andersen, Z.J., Oftedal, B.M., Stafoggia, M., Bellander, T., Strak, M., Wolf, K., Vienneau, D., Brunekreef, B., Hoek, G., 2020. Development of Europe-Wide Models for Particle Elemental Composition Using Supervised Linear Regression and Random Forest. Environ Sci Technol 54, 15698–15709. https://doi.org/10.1021/acs.est.0c06595

Coudon, T., Danjou, A.M.N., Faure, E., Praud, D., Severi, G., Mancini, F.R., Salizzoni, P., Fervers, B., 2019. Development and performance evaluation of a GIS-based metric to assess exposure to airborne pollutant emissions from industrial sources. Environmental Health 18, 8. https://doi.org/10.1186/s12940-019-0446-x

De Nicola, F., Spagnuolo, V., Baldantoni, D., Sessa, L., Alfani, A., Bargagli, R., Monaci, F., Terracciano, S., Giordano, S., 2013. Improved biomonitoring of airborne contaminants by combined use of holm oak leaves and epiphytic moss. Chemosphere 92, 1224–1230. https://doi.org/10.1016/j.chemosphere.2013.04.050

Di Palma, A., Capozzi, F., Spagnuolo, V., Giordano, S., Adamo, P., 2017. Atmospheric particulate matter intercepted by moss-bags: Relations to moss trace element uptake and land use. Chemosphere 176, 361–368. https://doi.org/10.1016/j.chemosphere.2017.02.120

Gall, J.E., Boyd, R.S., Rajakaruna, N., 2015. Transfer of heavy metals through terrestrial food webs: a review. Environ. Monit. Assess. 187, 201. https://doi.org/10.1007/s10661-015-4436-3

Gallego-Cartagena, E., Morillas, H., Carrero, J.A., Madariaga, J.M., Maguregui, M., 2021. Naturally growing grimmiaceae family mosses as passive biomonitors of heavy metals pollution in urban-industrial atmospheres from the Bilbao

Metropolitan area. Chemosphere 263, 128190. https://doi.org/10.1016/j.chemosphere.2020.128190

Gatto, N.M., Henderson, V.W., Hodis, H.N., St. John, J.A., Lurmann, F., Chen, J.-C., Mack, W.J., 2014. Components of air pollution and cognitive function in middle-aged and older adults in Los Angeles. NeuroToxicology 40, 1–7. https://doi.org/10.1016/j.neuro.2013.09.004

Genuis, S.J., Kelln, K.L., 2015. Toxicant Exposure and Bioaccumulation: A Common and Potentially Reversible Cause of Cognitive Dysfunction and Dementia. Behavioural Neurology 2015, e620143. https://doi.org/10.1155/2015/620143

Gnesin, G.G., 2013. On the Origin of Metallurgical Technologies in the Bronze Age. Powder Metall. Met. Ceram. 52, 477–488. https://doi.org/10.1007/s11106-013-9550-6

González, A.G., Pokrovsky, O.S., 2014. Metal adsorption on mosses: Toward a universal adsorption model. Journal of Colloid and Interface Science 415, 169–178. https://doi.org/10.1016/j.jcis.2013.10.028

Gräler, B., Pebesma, E., Heuvelink, G., 2016. Spatio-Temporal Interpolation using gstat. The R Journal 8, 204–218.

Grandjean, P., Landrigan, P.J., 2014. Neurobehavioural effects of developmental toxicity. The Lancet Neurology 13, 330–338. https://doi.org/10.1016/S1474-4422(13)70278-3

Harmens, H., 2010. MONITORING OF ATMOSPHERIC DEPOSITION OF HEAVY METALS, NITROGEN AND POPs IN EUROPE USING BRYOPHYTES. MONITORING MANUAL. International Cooperative Programme on Effects of Air Pollution on Natural Vegetation and Crops.

Harmens, H., Ilyin, I., Mills, G., Aboal, J.R., Alber, R., Blum, O., Coşkun, M., De Temmerman, L., Fernández, J.Á., Figueira, R., Frontasyeva, M., Godzik, B., Goltsova, N., Jeran, Z., Korzekwa, S., Kubin, E., Kvietkus, K., Leblond, S., Liiv, S., Magnússon, S.H., Maňkovská, B., Nikodemus, O., Pesch, R., Poikolainen, J., Radnović, D., Rühling, Å., Santamaria, J.M., Schröder, W., Spiric, Z., Stafilov, T., Steinnes, E., Suchara, I., Tabors, G., Thöni, L., Turcsányi, G., Yurukova, L., Zechmeister, H.G., 2012. Country-specific correlations across Europe between modelled atmospheric cadmium and lead deposition and concentrations in mosses. Environmental Pollution 166, 1–9. https://doi.org/10.1016/j.envpol.2012.02.013

Hiemstra, P.H., Pebesma, E.J., Twenhöfel, C.J.W., Heuvelink, G.B.M., 2008. Real-time automatic interpolation of ambient gamma dose rates from the Dutch Radioactivity Monitoring Network. Computers & Geosciences.

Hijmans, R.J., 2020. raster: Geographic Data Analysis and Modeling.

Institut national de la statistique et des études économiques (National Institute of Statistics and Economic Studies), n.d. Definition - IRIS | Insee [WWW Document]. URL https://www.insee.fr/en/metadonnees/definition/c1523 (accessed 9.7.21a).

Institut national de la statistique et des études économiques (National Institute of Statistics and Economic Studies), n.d. La grille communale de densité | Insee [WWW Document]. URL https://www.insee.fr/fr/information/2114627 (accessed 9.7.21b).

International Agency for Research on Cancer, 2016. IARC MONOGRAPHS ON THE EVALUATION OF CARCINOGENIC RISKS TO HUMANS (No. Volume 109). Lyon.

565 Jaworowski, Z., Bysiek, M., Kownacka, L., 1981. Flow of metals into the global
566 atmosphere. Geochimica et Cosmochimica Acta 45, 2185–2199.
567 https://doi.org/10.1016/0016-7037(81)90071-5
568 Jiang, Y., Fan, M., Hu, R., Zhao, J., Wu, Y., 2018. Mosses Are Better than Leaves of
569 Vascular Plants in Monitoring Atmospheric Heavy Metal Pollution in Urban
570 Areas. International Journal of Environmental Research and Public Health 15,
571 1105. https://doi.org/10.3390/ijerph15061105
572 Ledoux, F., Kfoury, A., Delmaire, G., Roussel, G., El Zein, A., Courcot, D., 2017.
573 Contributions of local and regional anthropogenic sources of metals in PM2.5
574 at an urban site in northern France. Chemosphere 181, 713–724.
575 https://doi.org/10.1016/j.chemosphere.2017.04.128
576 Lequy, E., Dubos, N., Witté, I., Pascaud, A., Sauvage, S., Leblond, S., 2017. Assessing
577 temporal trends of trace metal concentrations in mosses over France between
578 1996 and 2011: A flexible and robust method to account for heterogeneous
579 sampling strategies. Environmental Pollution 220, Part B, 828–836.
580 https://doi.org/10.1016/j.envpol.2016.10.065
581 Lequy, E., Sauvage, S., Laffray, X., Gombert-Courvoisier, S., Pascaud, A., Galsomiès,
582 L., Leblond, S., 2016. Assessment of the uncertainty of trace metal and
583 nitrogen concentrations in mosses due to sampling, sample preparation and
584 chemical analysis based on the French contribution to ICP-Vegetation.
585 Ecological Indicators 71, 20–31.
586 https://doi.org/10.1016/j.ecolind.2016.06.046
587 Lequy, E., Siemiatycki, J., Leblond, S., Meyer, C., Zhivin, S., Vienneau, D., de Hoogh,
588 K., Goldberg, M., Zins, M., Jacquemin, B., 2019. Long-term exposure to
589 atmospheric metals assessed by mosses and mortality in France. Environ Int
590 129, 145–153. https://doi.org/10.1016/j.envint.2019.05.004
591 Mailler, S., Menut, L., Khvorostyanov, D., Valari, M., Couvidat, F., Siour, G.,
592 Turquety, S., Briant, R., Tuccella, P., Bessagnet, B., Colette, A., Létinois, L.,
593 Markakis, K., Meleux, F., 2017. CHIMERE-2017: from urban to hemispheric
594 chemistry-transport modeling. Geoscientific Model Development 10, 2397–
595 2423. https://doi.org/10.5194/gmd-10-2397-2017
596 Markert, B., 2007. Definitions and principles for bioindication and biomonitoring of
597 trace metals in the environment. Journal of Trace Elements in Medicine and
598 Biology, Third International SymposiumFederation of European Societies on
599 Trace Elements and Minerals (FESTEM) 21, Supplement 1, 77–82.
600 https://doi.org/10.1016/j.jtemb.2007.09.015
601 Menut, L., Bessagnet, B., Khvorostyanov, D., Beekmann, M., Blond, N., Colette, A.,
602 Coll, I., Curci, G., Foret, G., Hodzic, A., Mailler, S., Meleux, F., Monge, J.-L.,
603 Pison, I., Siour, G., Turquety, S., Valari, M., Vautard, R., Vivanco, M.G., 2013.
604 CHIMERE 2013: a model for regional atmospheric composition modelling.
605 Geoscientific Model Development 6, 981–1028. https://doi.org/10.5194/gmd-
606 6-981-2013
607 Messager, M.L., Davies, I.P., Levin, P.S., 2021. Low-cost biomonitoring and high-
608 resolution, scalable models of urban metal pollution. Science of The Total
609 Environment 767, 144280. https://doi.org/10.1016/j.scitotenv.2020.144280
610 Natali, M., Zanella, A., Rankovic, A., Banas, D., Cantaluppi, C., Abbadie, L., Lata, J.-
611 C., 2016. Assessment of trace metal air pollution in Paris using slurry-TXRF
612 analysis on cemetery mosses. Environ Sci Pollut Res 23, 23496–23510.
613 https://doi.org/10.1007/s11356-016-7445-z
614 Neckel, A., Júnior, A.C.G., Ribeiro, L.A., Silva, C.C.O. de A., Cardoso, G.T., 2016.
615 Cemeteries heavy metals concentration analysis of soils and the contamination

risk for the surrounding resident population. International Journal of Engineering Research and Applications 6, 30–35.

Nordberg, G.F., Fowler, B.A., Nordberg, M. (Eds.), 2007. Handbook on the Toxicology of Metals. Elsevier. https://doi.org/10.1016/B978-0-12-369413-3.X5052-6

Schröder, W., Nickel, S., Schönrock, S., Meyer, M., Wosniok, W., Harmens, H., Frontasyeva, M.V., Alber, R., Aleksiayenak, J., Barandovski, L., Carballeira, A., Danielsson, H., Temmermann, L. de, Godzik, B., Jeran, Z., Karlsson, G.P., Lazo, P., Leblond, S., Lindroos, A.-J., Liiv, S., Magnússon, S.H., Mankovska, B., Martínez-Abaigar, J., Piispanen, J., Poikolainen, J., Popescu, I.V., Qarri, F., Santamaria, J.M., Skudnik, M., Špirić, Z., Stafilov, T., Steinnes, E., Stihi, C., Thöni, L., Uggerud, H.T., Zechmeister, H.G., 2016. Spatially valid data of atmospheric deposition of heavy metals and nitrogen derived by moss surveys for pollution risk assessments of ecosystems. Environ Sci Pollut Res 23, 10457–10476. https://doi.org/10.1007/s11356-016-6577-5

Schroeder, H.A., 1968. Airborne Metals. Scientist and Citizen 10, 83–88. https://doi.org/10.1080/21551278.1968.9957619

Tripathy, S., Tunno, B.J., Michanowicz, D.R., Kinnee, E., Shmool, J.L.C., Gillooly, S., Clougherty, J.E., 2019. Hybrid land use regression modeling for estimating spatio-temporal exposures to PM2.5, BC, and metal components across a metropolitan area of complex terrain and industrial sources. Sci Total Environ 673, 54–63. https://doi.org/10.1016/j.scitotenv.2019.03.453

Tyler, G., 1990. Bryophytes and heavy metals: a literature review. Botanical Journal of the Linnean Society 104, 231–253. https://doi.org/10.1111/j.1095-8339.1990.tb02220.x

Vieille, B., Albert, I., Leblond, S., Couvidat, F., Parent, É., Meyer, C., 2021. Are Grimmia Mosses Good Biomonitors for Urban Atmospheric Metallic Pollution? Preliminary Evidence from a French Case Study on Cadmium. Atmosphere 12, 491. https://doi.org/10.3390/atmos12040491

Zechmeister, H.G., Hohenwallner, D., Riss, A., Hanus-Illnar, A., 2005. Estimation of element deposition derived from road traffic sources by using mosses. Environ Pollut 138, 238–249. https://doi.org/10.1016/j.envpol.2005.04.005

Zins, M., Goldberg, M., Team, C., 2015. The French CONSTANCES population-based cohort: design, inclusion and follow-up. Eur J Epidemiol 30, 1317–1328. https://doi.org/10.1007/s10654-015-0096-4

- Airborne metal measures remain scarce to derive exposure for large urban populations
- We measured metals in mosses to derive exposure surfaces in two large French cities
- We applied land use regression modeling and obtained surfaces for 13 metals
- Models were satisfactory and robust particularly for cadmium and antimony

CRediT authorship contribution statement

Emeline Lequy: Conceptualization, Data Curation, Methodology, Software, Formal analysis, Writing - Original Draft, Writing - Review & Editing;

Caroline Meyer: Resources, Data Curation, Methodology, Writing - Review & Editing;

Danielle Vienneau: Methodology, Writing - Review & Editing

Claudine Berr: Funding acquisition, Writing - Review & Editing;

Marcel Goldberg: Funding acquisition, Writing - Review & Editing;

Marie Zins: Funding acquisition, Writing - Review & Editing;

Sébastien Leblond: Resources, Methodology; Funding acquisition, Writing - Review & Editing

Kees de Hoogh: Conceptualization, Supervision, Writing - Review & Editing

Bénédicte Jacquemin: Conceptualization, Funding acquisition, Supervision, Writing - Review & Editing

Declaration of interests

☒ The authors declare that they have no known competing financial interests or personal relationships that could have appeared to influence the work reported in this paper.

☐The authors declare the following financial interests/personal relationships which may be considered as potential competing interests: